Journal of Applied Polymer Science

Micro/Nanohybrid Hierarchical Poly(*N*-isopropylacrylamide)/Calcium Carbonate Composites for Smart Drug Delivery

Jun Shi, Wenyan Qi, Chao Du, Jin Shi, Shaokui Cao
School of Materials Science and Engineering, Zhengzhou University, Zhengzhou 450052, China
Correspondence to: J. Shi or S. Cao (shijun@zzu.edu.cn or caoshaokui@zzu.edu.cn)

ABSTRACT: Poly(*N*-isopropylacrylamide) (PNIPAAm)/calcium carbonate ($CaCO_3$) micro/nanohybrid composites with smart drug-delivery property had been prepared via *in situ* biomineralization reaction. Sodium poly(styrene sulfonate) (PSS) was used as the crystal growth additive to control the crystalline polymorph of $CaCO_3$ and the morphology of the hybrid materials. The interaction between PSS and Ca^{2+} contributed to the formation of hierarchical micro/nanohybrid composites, in which microscale vaterite microparticles were covered by nanoscale PNIPAAm micelle. Vitamin B_2 (VB_2) release behavior was found to be pH- and thermal-responsive. Moreover, the release profiles were sustained with the introduction of $CaCO_3$ microparticles, suggesting that $CaCO_3$ microparticles could hinder the permeation of the encapsulated VB_2 and reduce the drug release effectively. The prepared micro/nanohybrid materials can be used as "smart" hierarchical materials for controlled drug delivery. © 2012 Wiley Periodicals, Inc. J. Appl. Polym. Sci. 129: 577–584, 2013

KEYWORDS: Composites; self-assembly; drug-delivery systems; stimuli-sensitive polymers; biomimetic

Received 5 July 2012; accepted 11 October 2012; published online 3 November 2012
DOI: 10.1002/app.38718

INTRODUCTION

Poly(*N*-isopropylacrylamide) (PNIPAAm) is the most intensively studied smart polymer that exhibits remarkable hydration–dehydration changes in aqueous solution in response to small changes in temperature near its lowest critical solution temperature (LCST) around 32°C.[1–4] Many researchers have demonstrated that the rational mixing of polymeric nanogels with inorganic particles on a micro/nanoscale may result in the unusual properties.[5,6] Such polymeric/inorganic hybrid materials exhibit structural hierarchy and offer a unique combination of the properties with potential applications in drug-delivery systems and tissue-engineering fields.[7,8] Compared to single responsive drug carriers, drug carriers that can respond to more than one stimulus are very interesting owing to their physiological and biological applications.[9,10]

Previous studies have shown that organic/inorganic hybrid structure could improve the mechanical strength and controlled release behavior of polymer matrix.[11–13] Among these hybrid materials, calcium carbonate ($CaCO_3$)/polymer hybrid composites have shown promising potential for the development of smart drug carriers because of its ideal biocompatibility, biodegradability, and pH-sensitive properties.[14] It is widely accepted that $CaCO_3$ has three different anhydrous crystalline polymorphs: vaterite, aragonite, and calcite, with an increasingly thermodynamic stability. Recent advances in supermolecular assembly illustrate that micro/nanostructured $CaCO_3$/polymer hybrid materials can be used as drug carries in controlled drug delivery.[15–17] The combination of controlled $CaCO_3$ mineralization technique with the rational choice of polymer templates would lead to the successful development of smart and self-assembled drug carriers. Extensive studies have been reported concerning the synthesis of $CaCO_3$/polymer hybrid composites.[18,19] Moreover, much research has been done to prepare smart drug carriers using $CaCO_3$ as pH-sensitive component. For example, Wei et al.[20] fabricated hierarchical hollow $CaCO_3$ particles and applied these $CaCO_3$ particles as pH-sensitive anticancer drug carrier. In addition, previous studies have demonstrated the significant effect of the crystal growth additive on the nucleation and growth of $CaCO_3$ particles.[21,22] However, there have been few reports on the rational design of combination of $CaCO_3$ microparticles and thermal-responsive polymer by using crystal growth additive to prepare dual-responsive drug carriers.

Herein, we intend to combine the controlled $CaCO_3$ mineralization technique with the rational choice of polymer templates. A novel method for preparing hierarchical PNIPAAm/$CaCO_3$ micro/nanohybrid composites with controlled drug delivery is reported in the present study. Vitamin B2 was used as the model drug in this work. Vitamin B2 is a water-soluble drug.

Additional Supporting Information may be found in the online version of this article.

Applied Polymer SCIENCE

Moreover, the solubility of vitamin B2 is very good in acid condition. This is very important, because we must measure the dug content at different pH values (pH 2.1 and 7.4) in this work. PNIPAAm micelle nanotemplates were first prepared from *N*-isopropylacrylamide (NIPAAm) monomer via surfactant-free emulsion polymerization (described in Scheme 1). Then, PNIPAAm/$CaCO_3$ micro/nanohybrid materials were formed via the self-assembling of nanoscale PNIPAAm micelle around the surface of vaterite microparticles. Sodium poly(styrene sulfonate) (PSS) and poly(acrylic acid) (PAA; chemical structure was described in Scheme 2) were used as effective crystal growth additive to control the nucleation of microscale vaterite $CaCO_3$ microparticles. Vaterite microparticles could serve as a diffusion barrier for the encapsulated drugs, thereby producing robust micro/nanocarriers with controllable drug-release property. Such a compact hierarchical PNIPAAm/$CaCO_3$ hybrid structure could hinder the permeation of the encapsulated drug and endow the resulting hybrid composites with sustained release properties. Moreover, the thermosensitivity of PNIPAAm and pH-sensitivity of $CaCO_3$ microparticles would not be ruined after the mineralization process.

EXPERIMENTAL

Materials

NIPAAm (Tokyo Chemical Industry Co., Japan), potassium persulfate (KPS, Tianjin Sitong Chemical Reagent Co., China), *N*,*N*,*N*′,*N*′-tetramethylethylenediamine (Shanghai Chemical Regent Co., China), *N*,*N*-methylenebisacrylamide (MBA, Tianjin Chemical Reagent Institute, China), sodium PSS (M_w = 70,000, Alfa Organics), PAA (M_w = 2000, 63 wt % solution in water, Acros Organics), $(NH_4)_2CO_3$ (Tianjin Kemiou Chemical Reagent Institute, China), and vitamin B_2 (VB_2, Tianjin Damao Chemical, China) were used as received.

Preparation of $CaCO_3$/PNIPAAm Hybrid Composites

PNIPAAm micelle nanotemplates were prepared according to literature.[23] An aqueous solution was prepared by dissolving NIPAAm and MBA in deionized water. The solution was then degassed with nitrogen for 30 min. Afterward, KPS aqueous solution (2%) was added. After 2.5 h, 4.24 m*M* L^{-1} of PSS was added into the solution. After polymerizing for 6 h, the reactor was put into an ice bath. An appropriate amount of $CaCl_2$ (1.18, 2.27, and 3.55 m*M*) was dissolved directly in the solution. Thereafter, $(NH_4)_2CO_3$ was added dropwise to the above solution. The pH value of the solution was kept at nine by adjustment using NaOH (1 mol L^{-1}) solution. The reaction was kept for 1.5 h, and then 0.15 mg mL^{-1} of VB_2 was added. The obtained hybrid composites were extensively washed with distilled water and vacuum-dried for 48 h. Finally, 0.05 g of $CaCO_3$/PNIPAAm hybrid composites was compacted into a disk with a pressure of 10 MPa. Pure PNIPAAm nanogels as control samples were prepared under the same conditions in the absence of $CaCO_3$.

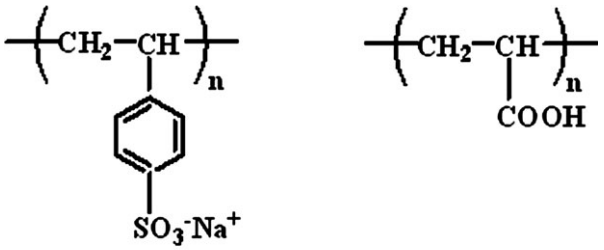

PSS PAA

Scheme 2. Chemical structure of PSS and PAA.

Characterization of Hybrid $CaCO_3$/PNIPAAm Composites

FTIR spectra were recorded with a Bruker Tensor 27 FTIR spectrometer in the range of 4000–500 cm^{-1} using KBr pellets. The morphology of the samples was observed using scanning electron microscopy (SEM, FEI Quanta 200) at an accelerated voltage of 20 kV. Before SEM observation, the samples were stabilized on aluminum stubs using adhesive and sputter-coated with an ~100 Å layer of gold. The high-magnification morphology of the samples was observed using field emission scanning electron microscope (FESEM, JEOL 7500F). Before FESEM observation, the samples were coated with an ~100 Å layer of platinum. The formation of $CaCO_3$ microcrystals in the hybrid

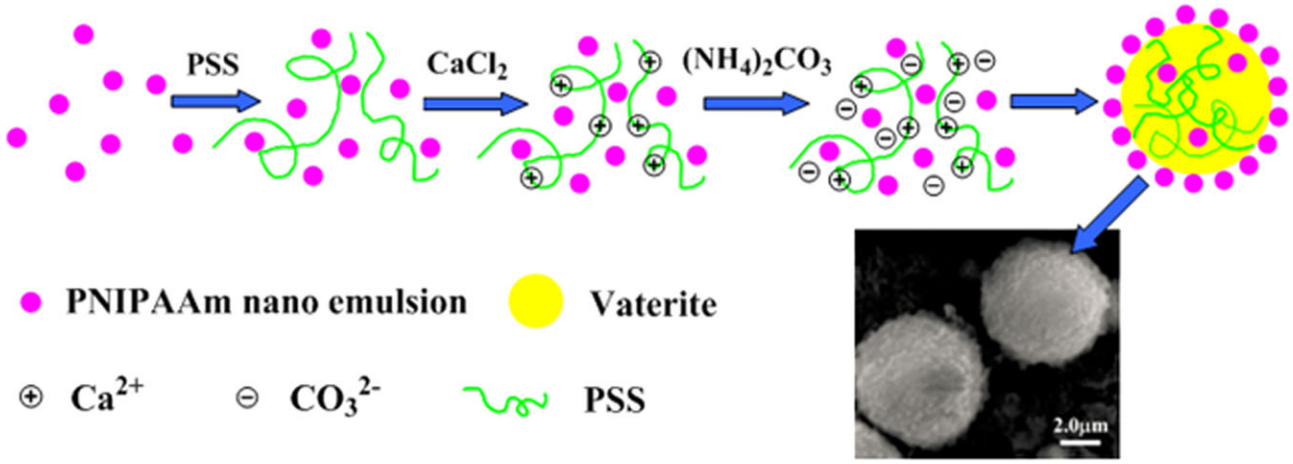

Scheme 1. Schematic illustration for the formation of the hybrid composites. [Color figure can be viewed in the online issue, which is available at wileyonlinelibrary.com.]

composites was confirmed by means of energy-dispersive X-ray spectrometer (EDX, INCA). The Brunauer-Emmett-Teller (BET) surface area of the samples was measured by using Micromeritics ASAP 2020 accelerated surface area and porosimetry system. Thermogravimetric analysis (TGA) was carried out on an STA 409 PC/PG simultaneous thermal analyzer (Netzsch) at a heating rate of 10°C min^{-1} under Ar atmosphere. X-ray power diffraction (XRD) patterns were recorded on a Rigaku D/MAX 2550 V X-ray diffractometer using Cu Ka radiation (λ= 1.54178 Å) with a graphite monochromator.

Determination of Drug Encapsulation Efficiency and *In Vitro* Release Studies

The prepared hybrid composites (10 mg) were dissolved in 100 mL of PBS with pH 7.4 under stirring during 24 h. The amount of free VB_2 was determined in the clear supernatant by UV spectrophotometry at 265 nm using the calibration curve constructed from a series of standard drug solutions, respectively. The loading efficiency is defined as the weight percentage of the loaded drug based on the feed amount.

The prepared hybrid composites (10 mg) were suspended in 50 mL of PBS with different pH value. The dissolution medium was stirred in a shaking bath. The sample (2 mL) was periodically removed, and the withdrawn amount was replaced by the same volume of fresh medium. These experiments were performed at least three times. The amount of released VB_2 was analyzed with a UV spectrophotometer as described previously.

RESULTS AND DISCUSSION

Characterization of Hybrid Composites

Hierarchical PNIPAAm/$CaCO_3$ micro/nanohybrid composites with sustained dual-responsive drug delivery had been prepared in the present work. Such an experimental design is based on the combination of vaterite microparticles with porous organic polymeric matrices. The compact hierarchical PNIPAAm/$CaCO_3$ hybrid structure could hinder the permeation of the encapsulated drug and endow the resulting hybrid composites with sustained release properties. Moreover, the thermosensitivity of PNIPAAm and pH-sensitivity of $CaCO_3$ microparticles would not be ruined after the mineralization process.

PSS is an effective additive to control the nucleation and growth of $CaCO_3$ microcrystals via the interaction between PSS and Ca^{2+}.[21,22] PSS could accelerate the transformation of $CaCO_3$ microparticles from calcite to vaterite. Previous studies have demonstrated the significant effect of PAA on the nucleation and growth of calcium phosphate.[24] In the present work, the effect of crystal growth additive (PSS and PAA) on the structure of PNIPAAm/$CaCO_3$ hybrid composites has also been discussed.

The prepared composites with different composition are listed in Table I. SEM micrographs of the hybrid composites are illustrated in Figure 1. The effect of crystal growth additive on the morphology of the hybrid composites can be seen in Figure 1. When using PSS as the crystal growth additive [Figure 1(A–C)], the size of $CaCO_3$ microparticles was around 1–2 μm for the composites prepared with 1.18 m*M* of $CaCl_2$ [Figure 1(A)]. However, the size of $CaCO_3$ microparticles prepared with 2.27 or 3.55 m*M* of $CaCl_2$ was around 4–5 μm as demonstrated by Figure 1(B,C). Another interesting phenomenon could be found from FESEM micrographs of the hybrid composites (Figure 2) that the surface of $CaCO_3$ microparticles was covered by a layer of PNIPAAm nanogels. The size of the PNIPAAm nanogels was around 200 nm. Then the EDX analyses were performed to confirm the composition of the resulting spherical composites [Figure 2(C,D)]. No signal of Ca element could be found, and the signal of N element was observed in the surrounding area of the spherical structure [location D in Figure 2(A)], suggesting that the nanogels scattering around the spherical structure were PNIPAAm nanogels. However, a strong signal for Ca element was observed for the outer layer of the spherical structure [location C in Figure 2(A)], indicating that the main component of inner spherical was $CaCO_3$ microparticles, and $CaCO_3$ microparticles were covered by PNIPAAm nanogels. Therefore, the successful combination of PNIPAAm nanogels with $CaCO_3$ microparticles could be demonstrated by FESEM and EDX analysis. In addition, as illustrated in Scheme 1, PNIPAAm nanogels were mixed homogeneously with PSS and Ca^{2+} in the initial stage of the composite formation. PNIPAAm nanogels would be inserted inside the vaterite microparticles during the course of biomineralization process. Therefore, we hypothesize that PNIPAAm nanogels would also exist inside the hybrid composites.

Table 1. Composition and Drug-Loading Efficiency of the Micro/Nanohybrid Composites

Sample	Crystal growth additive	Amount of $CaCl_2$ (mM)	Drug content (mg/10 mg sample)	Loading efficiency (%)
1		0	0.066 ± 0.04	21.29 ± 1.23
2	PSS	2.37	0.163 ± 0.03	61.43 ± 1.18
3	PSS	3.55	0.187 ± 0.01	79.98 ± 1.09
4	PSS	4.74	0.158 ± 0.02	77.02 ± 1.13
5	PAA	3.55	0.123 ± 0.03	53.93 ± 1.19

Compared to SEM micrographs of the hybrid composites prepared using different crystal growth additive, it could be found that the employment of PSS was benefited to prepare the vaterite microparticles [Figure 1(A–C)]. However, PNIPAAm micelle was not combined closely with the $CaCO_3$ microparticles [Figure 1(D)], and the $CaCO_3$ microparticles were nonspherical [arrows in the inset of Figure 1(D)] when using PAA as crystal growth additive. It is easier for vaterite phase than calcite phase to combine with PNIPAAm nanogels, which results the strong combination between vaterite and PNIPAAm nanogels.

As a dispersant, PSS can control the morphology of $CaCO_3$ particles and enhance their surface electric potential during the growth of $CaCO_3$ particles. Both PSS and PAA have long hydrophilic chains, because anionic functional groups such as sulfonate and carboxylate anions are connected on the long C—C main chains. However, PSS possesses rigid benzene side chains as described in Scheme 2. Sulfonate groups of PSS can complex with Ca^{2+} and disperse them to avoid agglomerating when $CaCO_3$ microparticles growing.[21,25] Moreover, steric hindrance of rigid benzene rings also has significant effect on

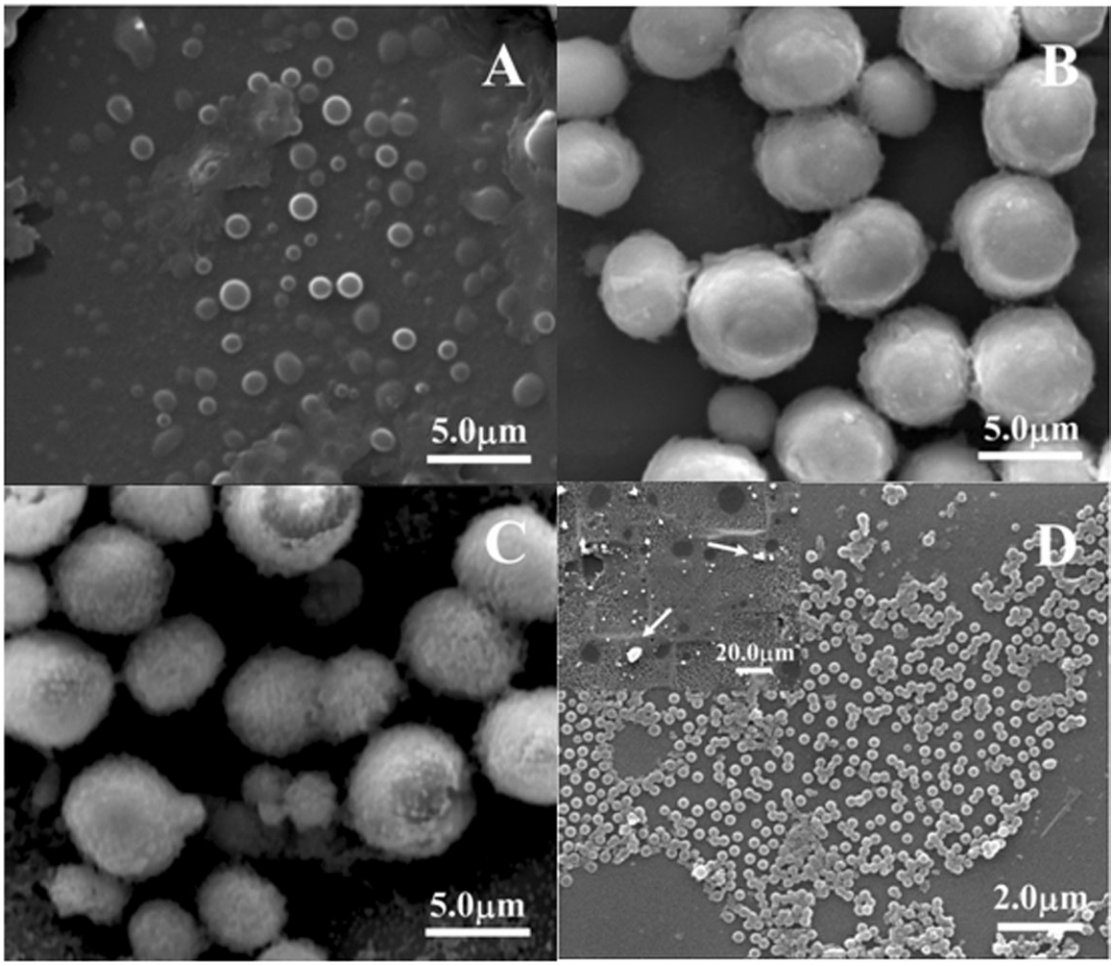

Figure 1. Effect of crystal growth additive on the morphology of PNIPAAm/$CaCO_3$ hybrid composites: hybrid composites using PSS as crystal growth additive prepared with 1.18 m*M* of Ca^{2+} (A), 2.37 m*M* of Ca^{2+} (B), 3.55 m*M* of Ca^{2+} (C), and hybrid composites using PAA as crystal growth additive prepared with 2.37 m*M* of Ca^{2+} (D).

hindering the aggregation of $CaCO_3$ microparticles. Therefore, negatively charged PSS assembled around the PNIPAAm nanogels would combine with Ca^{2+}, and microscale vaterite microparticles covered by nanoscale PNIPAAm micelle are formed. However, it is impossible for PAA to form spherical vaterite microparticles for the absence of rigid benzene side groups. It is clear that PSS plays a significant role to form the spherical vaterite microparticles.[25,26]

Figure 3(A) shows the Fourier transform infrared (FTIR) spectra of pure PNIPAAm nanogel and PNIPAAm/$CaCO_3$ hybrid composites prepared under different conditions. The absorbance of amide carbonyl groups in PNIPAAm was found at 1650 and 1567 cm^{-1}, the amide N—H bending appeared at 3075 and 2985 cm^{-1}. These signals could also be clearly detected in the hybrid composites prepared with 1.18 m*M* of Ca^{2+}, because the content of $CaCO_3$ was relatively low in this hybrid sample. The broad peaks at 875 cm^{-1} corresponding to the carbonyl (C—O) bond of calcite, vaterite, and aragonite could be observed in the hybrid composite,[27,28] indicating the formation of $CaCO_3$ microparticles after the hybridization reaction. Moreover, the broad peaks at 1475 cm^{-1} corresponding to the carbonyl (C=O) bond of vaterite could be observed for the hybrid composite prepared with 2.37 and 3.55 m*M* of Ca^{2+} using PSS as crystal growth additive. No obvious peaks at 1475 cm^{-1} could be found for the hybrid composite using PAA as crystal growth additive. These results indicate that PSS could control the nucleation and growth of $CaCO_3$ microparticles via the interaction between PSS and Ca^{2+} to form vaterite phase.

Figure 3(B) shows the XRD patterns of the PNIPAAm/$CaCO_3$ hybrid composites with different $CaCO_3$ contents. No typical XRD patterns of $CaCO_3$ microcrystals could be observed for the hybrid composites prepared with 1.18 m*M* of Ca^{2+} for the sake of the low-$CaCO_3$ content. For the hybrid composite prepared using PSS as crystal growth additive, typical XRD patterns of vaterite (labeled as *V*) could be assigned at 2θ of 21, 25, 27, and 33. However, for the hybrid composite using PAA as crystal growth additive, typical XRD patterns of calcite could be observed (labeled as C). FTIR and XRD results demonstrate that PSS plays the significant role to accelerate the transformation of $CaCO_3$ microparticles from calcite to vaterite and finally obtain spherical vaterite microparticles.

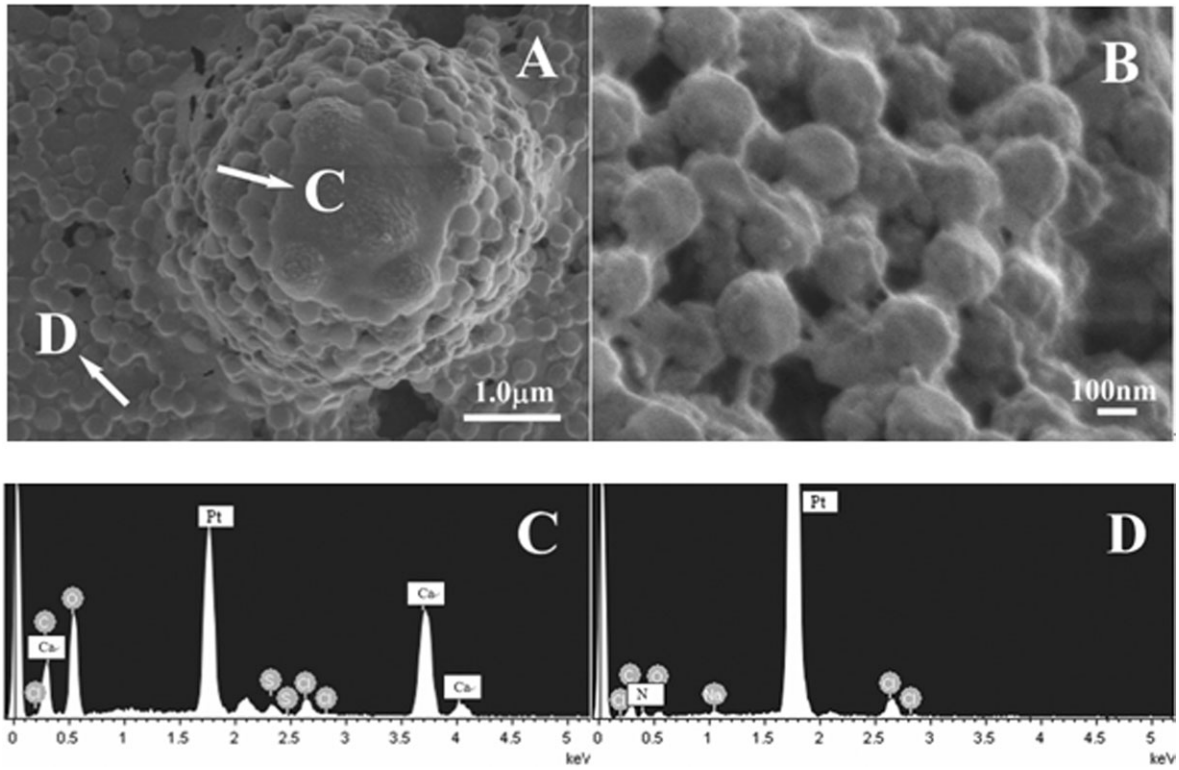

Figure 2. FESEM micrographs of PNIPAAm/$CaCO_3$ hybrid composites using PSS as crystal growth additive prepared with 2.37 m*M* of Ca^{2+} (A) and PNIPAAm nanogels in the surface of vaterite microparticles with high magnification (B). FESEM-associated EDX spectra of the surface of vetarite microparticles (C) and FESEM-associated EDX spectra of PNIPAAm nanogels in the near-surface regions of vetarite microparticles (D).

Figure 4 shows the thermogravimetric analyses of the PNIPAAm/$CaCO_3$ hybrid composites. The mass loss of the composites could be roughly divided into three regions. The mass loss below 150°C could be assigned to the loss of adsorbed water in the hybrid composites, the mass loss at 200–450°C was assigned to the decomposition of PNIPAAm nanogels,[20] and the mass loss at 500–800°C was assigned to the decomposition of $CaCO_3$ microparticles. It could also be observed that the weight percentages of residue for the hybrid composites prepared with 1.18 m*M* of Ca^{2+} were very low, suggesting that the $CaCO_3$ content was very low in this composite. The amounts of $CaCO_3$ in the composites prepared with higher Ca^{2+} concentrations (2.37 and 3.55 m*M*) were around 50% in weight. However, for samples prepared with 2.37 m*M* of Ca^{2+} using PAA as crystal growth additive, the $CaCO_3$ content was only 20%. PSS could accelerate the transformation of $CaCO_3$ microparticles from calcite to vaterite phase. It is easier for spherical vaterite than calcite to combine with PNIPAAm micelle, which results the strong combination between vaterite microparticles and PNIPAAm nanogels. Therefore, relatively higher $CaCO_3$ content could be obtained in the composites prepared with higher Ca^{2+} concentration.

As illustrated in Table I, the drug-loading efficiency of hybrid composites prepared with 1.18, 2.37, and 3.55 m*M* of Ca^{2+} using PSS as the crystal growth additive was 61.4, 80.0, and 77.1%, respectively. However, the value for PNIPAAm nanogels was only 21.3% and that for the composites using PAA as the crystal growth additive was 53.9%. As discussed in another literature,[18] vaterite phase could improve the stability of the PNIPAAm nanogels upon hybridization, which results the better combination among PNIPAAm nanogels, $CaCO_3$ microparticles, and VB_2. Therefore, the formation of PNIPAAm/$CaCO_3$ hybrid composites is a good method to prepare hydrophobic drug-loaded delivery materials.[23] Moreover, the BET surface area of PNIPAAm nanogel and PNIPAAm/$CaCO_3$ hybrid composites was 0.62 and 3.24 m^2/g, respectively. The data indicate that porous vaterite could increase the surface area of the PNIPAAm/$CaCO_3$ hybrid composites, which is benefited for the increasing of drug-loading efficiency and tailoring of smart drug delivery of the hybrid composites.

Swelling Study

$CaCO_3$ microparticles would be rapidly dissolved, and the composites were broken into fragments after 1 h at pH 2.1. Therefore, no valuable swelling ratio data could be obtained at pH 2.1 for prepared samples. We took the digital photographs of the hybrid composites at pH 2.1 and 7.4 for different period. As illustrated in Supporting Information Figure S1 of ESI, the composites immersed at pH 7.4 would be slightly swollen after several hours. However, the composites would be broken into fragments after 1 h, and the total quantity of the fragments would decrease after 5 h when immersing at pH 2.1, indicating that $CaCO_3$ microcrystallines had been dissolved.

Figure 5(A) shows the swelling behavior of the hybrid composites and pure PNIPAAm nanogels at pH 7.4 and 37°C. The swelling ratio of pure PNIPAAm nanogels was much higher

Applied Polymer SCIENCE

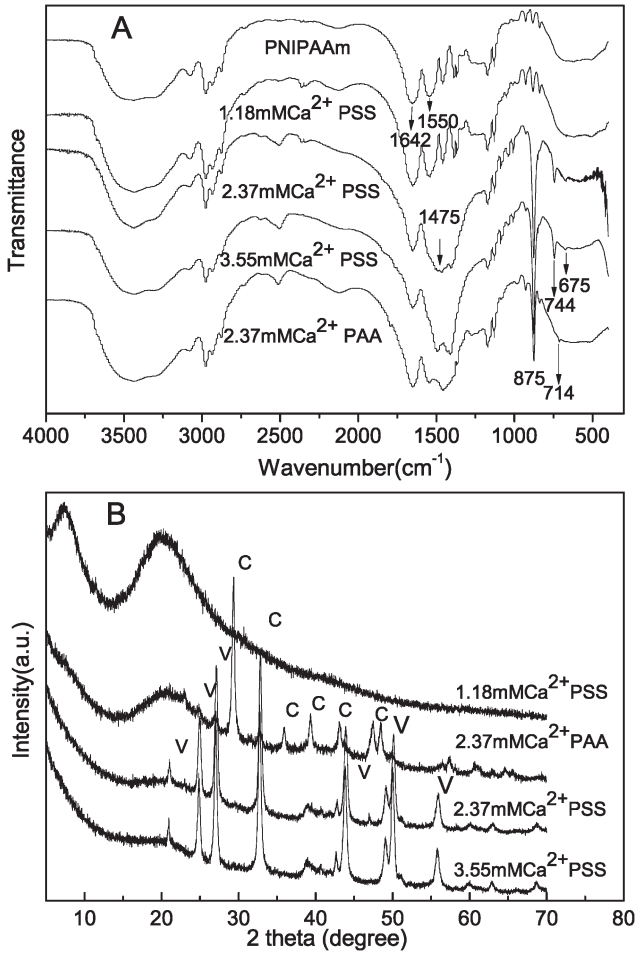

Figure 3. FTIR spectra of PNIPAAm, PNIPAAm/$CaCO_3$ hybrid composites prepared with different conditions (A) and XRD curves of the hybrid composites (B). "C" denotes for the calcite phase and "V" denotes for the vaterite phase in (B).

than that of PNIPAAm/$CaCO_3$ hybrid composites at pH 7.4 and 37°C. The combination of $CaCO_3$ microparticles with PNIPAAm nanogels would inhibit the extension of the polymer chain and then suppress the swelling ratio.[29,30] Moreover, the swelling ratio of hybrid composites at 25°C was higher than that at 37°C, indicating the shrinkage of PNIPAAm polymeric chains above its LCST. The swelling property will affect the drug-release properties of the hybrid composites, which will be discussed in the following.

Sustained Release

Figure 5(B) shows the VB_2 release profiles of the hybrid composites prepared using PSS as crystal growth additive and pure PNIPAAm nanogels measured at 37°C and pH 7.4. The drug release was around 91% after 12 h for pure PNIPAAm nanogels; however, the value for the composites prepared with 2.37 and 3.55 m*M* of Ca^{2+} was only 82%. For the hybrid composites prepared with 1.18 m*M* of Ca^{2+}, the drug release was as fast as that of pure PNIPAAm nanogels, suggesting that low content of $CaCO_3$ microparticles could not successfully decrease the permeability of VB_2 and then the drug release. It must be noted

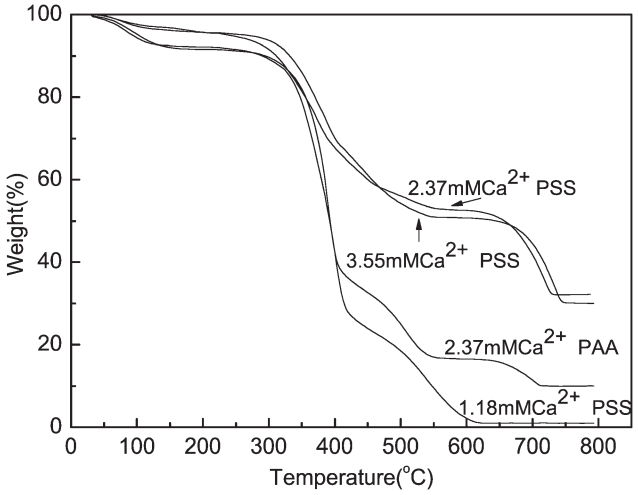

Figure 4. TG curves of PNIPAAm/$CaCO_3$ hybrid composites prepared with different conditions.

from Figure 5(B) that the initial burst release of pure PNIPAAm nanogels had been modified after hybridization process. The drug-release property of the hybrid composites is in line with

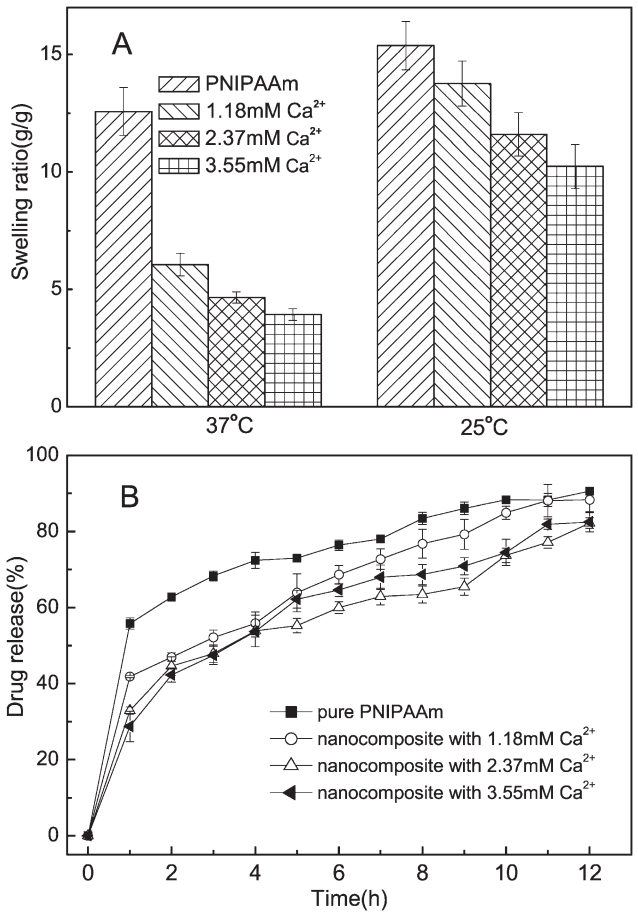

Figure 5. Equilibrium swelling ratio (A) and sustained drug release profiles measured at 37°C and pH 7.4 (B) of the hybrid composites using PSS as crystal growth additive.

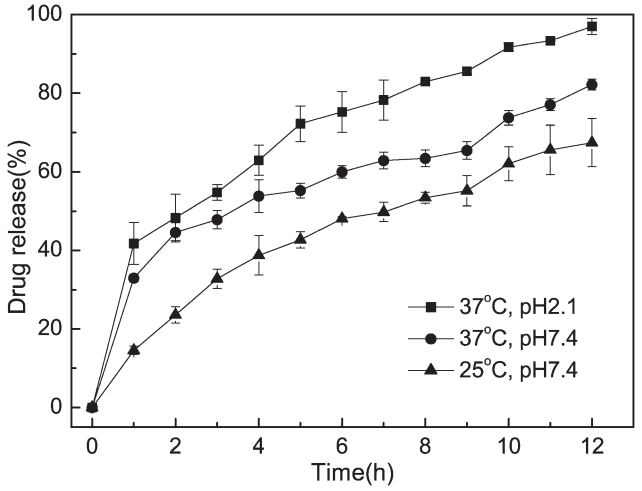

Figure 6. pH- and thermal-dependent release profiles of the hybrid composites prepared with 2.37 m*M* of Ca^{2+} using PSS as crystal growth additive.

the morphology and swelling results. The hybridization of pure PNIPAAm nanogels with suitable content of $CaCO_3$ microparticles could hinder the permeability of the encapsulated drug and reduce the drug release effectively.[31] A Student's *t*-test analysis was conducted to support this point; the *P* values between the data of pure PNIPAAm nanogels and that of the composites prepared with 2.37 m*M* of Ca^{2+} were less than 0.0031 within 12 h. The difference between these data was very statistically significant (greater than 95% confidence) for the considered time period.

Drug-release profiles of the hybrid composites using PSS and PAA as crystal growth additive measured at 37°C and pH 7.4 were presented in Supporting Information Figure S2 of ESI. Student's *t*-test analysis showed that the difference between the drug release of the hybrid composites using PSS and PAA as crystal growth additive was not statistically different (*P* values was 0.9017, greater than 95% confidence), indicating that the crystal type of $CaCO_3$ microparticles had little effect on the drug-release behavior of PNIPAAm/$CaCO_3$ hybrid composites.

Temperature/pH-Sensitive Release

Figure 6 presents the smart drug-release profiles for PNIPAAm/$CaCO_3$ hybrid composites using PSS as crystal growth additive at different pH values and temperatures. $CaCO_3$ microparticles are relatively insoluble at physiological pH value but have increasing solubility in acidic environments. This pH-dependent solubility endows the prepared hybrid materials with pH-sensitivity property.[12,20] The drug release was 97% after 12 h at pH 2.1, whereas the value was only 81% at pH 7.4 with the same treatment, suggesting a good response to the pH value for the prepared hybrid composites. Student's *t*-test analysis showed that the difference between the drug release of the PNIPAAm/$CaCO_3$ hybrid composites at pH 2.1 and 7.4 was statistically different (*P* values was 0.0503, greater than 95% confidence). The relatively high release at pH 2.1 should be related to the fast dissolution of vaterite microparticles at lower pH, which results in the quick diffusion of the drug within the hybrid composites.[12,32]

A temperature-dependent response was also clearly observed from Figure 6. The drug release at 37°C was 82%, which was 15% higher than that at 25°C (67%) after 12 h. Student's *t*-test analysis showed that the difference between the release of the hybrid composites at 37 and 25°C was statistically different (*P* values were 0.0389, greater than 95% confidence). The shrinkage of PNIPAAm nanogels in the surface of the hybrid composites would damage the compact surface structure of the composites and then accelerate the drug release from the hybrid composites at 37°C. Moreover, the squeezing of PNIPAAm nanogels inside the hybrid composites at 37°C can also break the balance of the hybrid composites and then accelerate the disruption of the composites.[33–35] The pH- and thermal-responsive properties indicate that PNIPAAm/$CaCO_3$ hybrid composites could hinder the permeation of the encapsulated drug and reduce the drug release effectively and preserve the thermosensitivity of PNIPAAm and pH-sensitivity of $CaCO_3$ microparticles after the mineralization process at the same time.

CONCLUSIONS

A novel method for preparing hierarchical PNIPAAm/$CaCO_3$ micro/nanohybrid composites with sustained dual-responsive drug delivery had been reported in the present work. The interaction between negatively charged PSS and positively charged Ca^{2+} could inhibit the aggregation of $CaCO_3$ microparticles, and finally microscale vaterite microparticles covered by nanoscale PNIPAAm nanogels could be obtained upon hybridization by using PSS as a crystal growth additive. SEM and EDX results demonstrated the formation of the hierarchical micro/nano-PNIPAAm/$CaCO_3$ hybrid composites. VB_2 release behaviors of the hybrid composites revealed that vaterite microparticles could hinder the permeation of the encapsulated drug and endow the hybrid composites with sustained release properties and preserve the thermo- and pH-sensitivity of the hybrid composites at the same time.

ACKNOWLEDGMENTS

This work was financially supported by the National Natural Science Foundation of China (Project 20874090).

REFERENCES

1. Jaiswal, M. K.; Mehta, S.; Banerjee, R.; Bahadur, D. *Colloid Polym. Sci.* **2012**, *290*, 607.
2. Petrusic, S.; Lewandowski, M.; Giraud, S.; Jovancic, P.; Bugarski, B.; Ostojic, S.; Koncar, V. *J. Appl. Polym. Sci.* **2012**, *124*, 890.
3. Agrawal, M.; Gupta, S.; Stamm, M. *J. Mater. Chem.* **2011**, *21*, 615.
4. Shi, J.; Alves, N. M.; Mano, J. F. *Adv. Funct. Mater.* **2007**, *17*, 3312.
5. Marinakos, S. M.; Shultz, D. A.; Feldheim, D. L. *Adv. Mater.* **1999**, *11*, 34.
6. Beecroft, L. L.; Ober, C. K. *Chem. Mater.* **1997**, *9*, 1302.

7. Gupta, S.; Agrawal, M.; Uhlmann, P.; Simon, F.; Stamm, M. *Chem. Mater.* **2010**, *22*, 504.
8. Agrawal, M.; Rubio-Retama, J.; Zafeiropoulos, N. E.; Gaponik, N.; Gupta, S.; Cimrova, V.; Lesnyak, V.; Lopez-Cabarcos, E.; Tzavalas, S.; Rojas-Reyna, R.; Eychmuller, A.; Stamm, M. *Langmuir* **2008**, *24*, 9820.
9. Yuan, Q. C.; Cayre, O. J.; Fujii, S.; Armes, S. P.; Williams, R. A.; Biggs, S. *Langmuir* **2010**, *16*, 18408.
10. Berger, S.; Zhang, H. P.; Pich, A. *Adv. Funct. Mater.* **2009**, *19*, 554.
11. Kakizawa, Y.; Miyata, K.; Furukawa, S.; Kataoka, K. *Adv. Mater.* **2004**, *16*, 699.
12. Epple, M.; Ganesan, K.; Heumann, R.; Klesing, J.; Kovtun, A.; Neumann, S.; Sokolova, V. *J. Mater. Chem.* **2010**, *20*, 18.
13. Rivera, G. P.; Parak, W. J. *ACS Nano.* **2008**, *2*, 2200.
14. Sokolova, V.; Epple, M. *Angew. Chem. Int. Ed.* **2008**, *47*, 1382.
15. Hu, L.; Mao, Z. W.; Gao, C. Y. *J. Mater. Chem.* **2009**, *19*, 3108.
16. Zhang, M. Z.; Kazunori, K. *Nano. Today* **2009**, *4*, 508.
17. Lee, H. J.; Kim, S. E.; Kwon, I. K.; Park, C.; Yang, C. J. K.; Lee, S. C. *Chem. Commun.* **2010**, *46*, 377.
18. Fukui, Y.; Fujimoto, K. *J. Mater. Chem.* **2012**, *22*, 3493.
19. Wakayama, H.; Hall, S. R.; Fukushima, Y.; Mann, S. *Ind. Eng. Chem. Res.* **2006**, *45*, 3332.
20. Wei, W.; Ma, G. H.; Hu, G.; Yu, D.; Mcleish, T.; Su, Z. G.; Shen, Z. Y. *J. Am. Chem. Soc.* **2008**, *130*, 15808.
21. Jin, Y.; Liu, W. C.; Wang, J. R.; Fang, H. J.; Gao, H. Q. *Colloid. Surf. A* **2009**, *342*, 40.
22. Wang, Y. S.; Moo, Y. X.; Chen, C. P.; Gunawan, P.; Xu, R. *J. Colloid. Interf. Sci.* **2010**, *352*, 393.
23. Shi, J.; Qi, W. Y.; Li, G. F.; Cao, S. K. *Mater. Sci. Eng. C* **2012**, *32*, 1299.
24. Shi, J.; Zhang, Z. Z.; Li, G. F.; Cao, S. K. *J. Mater. Chem.* **2011**, *21*, 16028.
25. Jada, A.; Verraes, A. *Colloid. Surf. A* **2003**, *219*, 7.
26. Xu, X. R.; Caia, A. H.; Liu, R.; Pan, H. H.; Tang, R. K.; Cho, K. *J. Crystal Growth* **2008**, *310*, 3779.
27. Guo, X. H.; Liu, L.; Wang, W.; Zhang, J.; Wang, Y. Y.; Yu, S. H. *CrystEngComm* **2011**, *13*, 2054.
28. Quan, C. Y.; Wu, D. Q.; Chang, C.; Zhang, G. B.; Cheng, S. X.; Zhang, X. Z.; Zhuo, R. X. *J. Phys. Chem. C* **2009**, *113*, 11262.
29. Shi, J.; Zhang, Z. Z.; Qi, W. Y.; Cao, S. K. *Int. J. Biol. Macromol.* **2012**, *50*, 747.
30. Shi, J.; Liu, X. P.; Shang, Y. J.; Cao, S. K. *J. Membr. Sci.* **2010**, *352*, 262.
31. Cao, S. W.; Zhu, Y. J.; Wu, J.; Wang, K. W.; Tang, Q. L. *Nanoscale Res. Lett.* **2010**, *5*, 781.
32. Ewence, A. E.; Bootman, M.; Roderick, H. L.; Skepper, J. N.; McCarthy, G.; Epple, M.; Neumann, M.; Shanahan, C. M.; Proudfoot, D. *Circ. Res.* **2008**, *103*, E28.
33. Sun, X. M.; Shi, J.; Zhang Z. Z.; Cao, S. K. *J. Appl. Polym. Sci.* **2011**, *122*, 729.
34. Wei, H.; Zhang, X. Z.; Cheng, H.; Chen, W. Q.; Cheng, S. X.; Zhuo, R. X. *J. Control. Release* **2006**, *116*, 266.
35. Gil, E. S.; Hudson, S. M. *Prog. Polym. Sci.* **2004**, *29*, 1173.